

An improved method to quantify bulk carbohydrate in marine planktonic samples

Ying-Yu Hu ^{1*}, Andrew J. Irwin ², Zoe V. Finkel¹

¹Department of Oceanography, Dalhousie University, Halifax, Nova Scotia, Canada

²Department of Mathematics & Statistics, Dalhousie University, Halifax, Nova Scotia, Canada

Abstract

The TPTZ (2,4,6-tripyridyl-s-triazine) method is used to detect monosaccharides from seawater and particulate matter samples because it is sensitive, precise, rapid and easy to perform. Contrary to mechanisms proposed in the literature, we provide evidence that the TPTZ method detects hydroxyl as well as aldehyde groups in monosaccharides when all reducing groups are fully deprotonated in alkaline medium. We use this insight to develop an optimized hydrolysis protocol to increase yields from polysaccharides while minimizing the dehydration of monosaccharides. Compared to the TPTZ method with commonly used hydrolysis protocols and the often-used phenol-sulfuric acid method, our new optimized method detects a wider range of carbohydrates with a more consistent yield relative to glucose and much lower coefficient of variation. When applied to phytoplankton cultures and marine particulate samples, our new method achieves significantly higher bulk carbohydrate yields.

There is a pressing need for reliable methods to quantify bulk and specific carbohydrates. Carbohydrates represent a substantial portion of the organic carbon pool, encompassing thousands of distinct molecules that range from simple sugars to complex structural components of living organisms. Carbohydrate molecules store energy (Deschamps et al. 2008; Ramli et al. 2020), fuel the growth and metabolic activities of microorganisms (Amosti et al. 2021; Priest et al. 2023), and form crucial structural components such as cell walls, matrices, and extracellular transparent exopolymer particles (Passos et al. 2015; Latil de Ros 2017). In marine ecosystems, phytoplankton carbohydrates, including mono-, oligo-, and polysaccharides, account for 10–75% of the total particulate carbon pool (Becker et al. 2020). Phytoplankton carbohydrate composition varies across species, growth stages, and environmental conditions (Biersmith and Benner 1998; Fearon 2014). Extracellular algal glycans may affect carbon sequestration in the ocean by modulating organic carbon degradation by bacteria (Bligh et al. 2022). Quantifying phytoplankton carbohydrates and their contribution to the organic carbon pool is essential for researchers to gain a comprehensive understanding of marine carbon cycling and ecosystem functioning.

*Correspondence: ruby.hu@dal.ca

This is an open access article under the terms of the [Creative Commons Attribution-NonCommercial-NoDerivs](https://creativecommons.org/licenses/by-nc-nd/4.0/) License, which permits use and distribution in any medium, provided the original work is properly cited, the use is non-commercial and no modifications or adaptations are made.

Carbohydrate quantification involves two primary approaches: specific methods targeting individual carbohydrate molecules and assays measuring the overall bulk (undifferentiated) carbohydrate pool. Targeted methods, such as high-performance liquid chromatography, high-performance anion exchange chromatography with pulsed amperometric detection, gas chromatography–mass spectrometry, Fourier-transform infrared spectroscopy, and nuclear magnetic resonance (NMR) focus on separating and detecting specific classes of molecules (Schievano et al. 2017). Newer methods use antibodies or enzymes to detect specific polysaccharides (Becker et al. 2020; Vidal-Melgosa et al. 2021). The quantification of bulk carbohydrate pool often relies on colorimetric methods, including: the phenol-sulfuric acid (PSA) method, the 3-methyl-2-benzothiazolinone hydrazone (MBTH) method, and the 2,4,6-tripyridyl-1,3,5-triazine (TPTZ) method, and more rarely, methods such as solid-state ¹³C NMR have been used (Hedges et al. 2001). The PSA method, initially developed by Dubois et al. (1951) for analyzing single monosaccharides and later extended to the bulk pool (Romankevich and Artem'ev 1969), uses concentrated H₂SO₄ to hydrolyze oligo- and polysaccharides into constituent monosaccharides. Subsequently, both the free and liberated monosaccharides undergo dehydration, forming different furfural derivatives depending on the type of monosaccharide. These derivatives react with phenol, producing orange-yellow–gold-colored compounds with absorbance peaks

around 480–490 nm. The variable molar absorptivity from furfural derivatives is compared to one standard, typically glucose. Therefore, the PSA method often yields substantial variation in recovery, ranging from 35% for L-fucose to 100% for D-xylose (Handa 1966). Consequently, this method is prone to substantial mis-quantification (van Wychen et al. 2017) and is considered semi-quantitative (van Oijen et al. 2005). Despite these well-known limitations, the PSA method remains widely used due to its simplicity and cost-effectiveness (Tornabene et al. 1985; Brown 1991; Lee et al. 2016; Becker et al. 2020; Niaz et al. 2020; Andreeva et al. 2021; Chen et al. 2023).

The MBTH and TPTZ methods are alternative colorimetric approaches for quantifying monosaccharides, offering more consistent recoveries of a range of carbohydrates compared to the PSA method. The MBTH method, as described by Burney and Sieburth (1977) and Pakulski and Benner (1992), quantifies the blue complex ($\lambda_{\max} = 635$ nm) formed by MBTH and formaldehyde following aldehyde reduction by potassium borohydride, originating from the oxidation of alditols via periodic acid (Hickey 2012). It generally yields relatively consistent recovery rates between 83% and 107% for most monosaccharides. Uronic acid recovery is incomplete due to partial lactonization of the carboxylic acid moiety, leading to an irreproducible alditol (Fazio et al. 1982). The TPTZ method, described by Myklestad et al. (1997), measures a navy blue complex ($\lambda_{\max} = 595$ nm) formed through the reaction of TPTZ and ferrocyanide, following the reduction of ferricyanide by aldehyde (Avigad 1975; Hickey 2012). While this method is rapid and generally provides acceptable recovery rates (88–103%), recovery rates for deoxysugars and uronic acid are low and the exact reason for this discrepancy is not fully understood.

Measurement methods targeting specific carbohydrate molecules or bulk carbohydrate with the MBTH and TPTZ methods only detect monosaccharides. To measure total carbohydrate content, oligo- and polysaccharides must be hydrolyzed into their constituent monosaccharides. Mild acid hydrolysis often falls short in fully releasing monosaccharides from complex biological or environmental samples, leading to an underestimation of bulk carbohydrates, while concentrated acid hydrolysis can increase or decrease carbohydrate yield. Studies have shown that the recovery of monosaccharides decreases with an increase in acid molarity beyond 0.8 mol L⁻¹ HCl (Engel and Händel 2011), and the absorbances of mono- and polysaccharide standards decreased after sulfuric acid hydrolysis (Pakulski and Benner 1992; Chanudet and Filella 2006). Borch and Kirchman (1997) observed the destruction of ribose and fructose after 4–24 h of hydrolysis in 0.85 mol L⁻¹ H₂SO₄, possibly due to dehydration. A two-step sulfuric acid hydrolysis using 12 mol L⁻¹ H₂SO₄ (Mopper 1977) has been shown to significantly increase carbohydrate recovery from dissolved and particulate carbohydrates in seawater, relative to hydrolysis by weak hydrochloric acid (Pakulski and Benner 1992). We

propose that low carbohydrate recovery after hydrolysis might be due to varying degrees of dehydration during hydrolysis. In the colorimetric assays, strong acids reduce monosaccharide functional groups, decreasing the yield of colored complexes, giving lower molar absorptivity and as a result, lower recovery. In the methods targeting specific molecules, the loss of functional groups from monosaccharides produces complex derivatives, which are challenging to identify. An understanding of the chemistry behind carbohydrate hydrolysis is crucial for developing an optimized method that efficiently cleaves the glycosidic bonds in oligo- and polysaccharides while preserving the molecular structure of monosaccharides.

The TPTZ analysis of carbohydrate is based on the formation of the colored TPTZ-Fe²⁺ complex produced by ferrocyanide reduced from ferricyanide. Myklestad et al. (1997) proposed that ferricyanide was reduced by aldehyde in reducing sugars: $\text{RCHO} + 2\text{Fe}(\text{CN})_6^{3-} + 3\text{OH}^- \rightarrow \text{RCO}_2^- + 2\text{Fe}(\text{CN})_6^{4-} + 2\text{H}_2\text{O}$. Since hydrolyzed and unhydrolyzed monosaccharides both have a single aldehyde group, recovery across sugars and hydrolysis conditions should exhibit little variation with this mechanism. Here, we observe variation in recovery from different types of monosaccharides, indicating that the TPTZ method detects hydroxyl groups in addition to aldehyde. We use the TPTZ method to compare changes in the number of reducing group lost during different hydrolysis protocols. It is important to note that the pH of the hydrolysate used in the TPTZ method can also affect total carbohydrate recovery, as complete deprotonation of all reducing groups is necessary for a complete reduction reaction of ferricyanide.

In this paper, we evaluate our hypothesis that hydroxyl groups as well as aldehyde contribute to the reduction of ferricyanide to ferrocyanide in the TPTZ method. We investigate the optimal amount of base required for consistent hydrolysate alkalization to achieve complete color development and quantitation of the TPTZ-Fe²⁺ complex. Through UV spectroscopy, we examine the effects of harsh acid hydrolysis on monosaccharide dehydration. Subsequently, we develop a hydrolysis protocol that balances monosaccharide dehydration and liberation from oligo- and polysaccharides by testing various hydrolysis conditions (acid type, concentration, duration, temperature) on common mono-, oligo-, and polysaccharides. We use these results to design an optimized protocol for hydrolysis and the TPTZ reaction to enable quantitation of mixed carbohydrate samples that is predictable, repeatable, and reliable.

Materials and procedures

Glassware and the cleaning procedures

Amber glass vials for the TPTZ reaction (12 mL; B7800-12A; Thermo Fisher Scientific) and glass centrifuge tubes for hydrolysis (10 mL; Corning® 99502-10 PYREX®) were cleaned with phosphate free detergent then with 5% vol vol⁻¹ hydrochloric

acid, thoroughly rinsed with reverse osmosis water and then pre-combusted at 500°C for 6 h before use.

Reagents, carbohydrate standards, and phytoplankton samples

Water used for standards and phytoplankton media preparation was purified to 18.2 M Ω using a Direct 16 Millipore unit. Reagents including concentrated sulfuric acid (18 mol L⁻¹), sodium hydroxide, sodium carbonate, sodium acetate, ferric chloride hexahydrate, potassium ferricyanide(III), citric acid and acetic acid were of ACS grade. TPTZ (2,4,6-tripyridyl-s-triazine, T1253) was obtained from Sigma-Aldrich. Most carbohydrate standards were obtained from Sigma-Aldrich, including D-(+)-glucose (G8270), D-(+)-mannose (63580), D-(+)-galactose (G0750), D-(-)-fructose (F0127), L-(+)-rhamnose (R3875), D-(+)-fucose (F8150), D-(+)-xylose (95729), L-(+)-arabinose (A3256), D-glucuronic acid (G5269), D-(+)-galacturonic acid (92478), D-mannuronic acid (SMB00280), N-acetyl-D-glucosamine (A8625), sucrose (S7903), raffinose (83400), α -cellulose (C6429), laminarin (L9634), amylose (A0512), pectin (P9135), chitin (C9752), and alginate (A1112). D-(-)-ribose (AC132360050) was obtained from Fisher Scientific. All carbohydrate standards were assessed in three replicates with an associated Milli-Q blank. Three concentrations (500 μ L of 100, 200, and 400 μ g mL⁻¹) of monosaccharides and water-soluble polysaccharides (laminarin and alginate) were added to glass centrifuge tubes. Around 50, 100, or 200 μ g dry powder of cellulose, amylose, pectin, and chitin was weighed and suspended in 500 μ L Milli-Q.

Particulate carbohydrate was analyzed from three lab-cultured phytoplankton species: the coccolithophore *Emiliania huxleyi* (RCC1266), the diatom *Thalassiosira pseudonana* (CCMP1335), and the diatom *Minutocellus polymorphus* (CCMP501). *E. huxleyi* (RCC1266) was grown at 20°C and 280 μ mol photons m⁻² s⁻¹ with a 12 : 12 h light-dark cycle in L/25 medium (Hallegraeff et al. 2004) using an aged sterilized natural seawater base with 43.8 μ mol L⁻¹ nitrate and 0.896 μ mol L⁻¹ phosphate under 41.10 and 2.7 Pa (1 atm \approx 10 μ atm) pCO₂. *T. pseudonana* (CCMP1335) was grown at 20°C and 200 μ mol photons m⁻² s⁻¹ with a continuous light cycle in an enriched artificial seawater (Berges et al. 2001). *M. polymorphus* (CCMP501) was grown at 20°C and 60 μ mol photons m⁻² s⁻¹ with a 12 : 12 h light-dark cycle in f/2 medium (Guillard and Ryther 1962) using an aged sterilized natural seawater base. Eight replicate phytoplankton samples were collected on 25 mm glass fiber filters (GF/F) (pre-combusted at 450°C for 4 h), using gentle vacuum pressure (130 mmHg) at the mid-exponential phase of growth. Duplicate sample blanks were GF/F filters with phytoplankton media filtered through them.

Particulate seawater samples were collected in acid-cleaned sample bottles from 1-m-depth at 44°41'37"N, 63°38'25"W (Bedford Basin, NS, Canada) on 31 March 2022. Back in the lab, 500 mL was filtered on 25 mm GF/F (pre-combusted at 450°C for 4 h), using gentle vacuum pressure (130 mmHg).

Samples were collected in eight replicates. Duplicate pre-combusted GF/F without sample were used as blanks.

All phytoplankton samples and blanks were flash frozen in liquid nitrogen and stored at -80°C. Before measurement, samples were freeze-dried. Samples and their associated blank filters were then transferred into 10 mL glass centrifuge tubes and 500 μ L Milli-Q was added before hydrolysis. To test if freeze drying resulted in a loss of carbohydrate, we prepared standards in solutions, freeze-dried them, and reconstituted them into solutions for measurement. We observed no change in the concentration of standards within the assay range we used. Crompton (2006) also reported complete recovery of glucose obtained from water after freeze-drying.

Monosaccharide hydrolysis: Sulfuric acid concentration, duration, and incubation temperature

To identify sulfuric acid concentrations that can cause dehydration in monosaccharide hydrolysis, glucose standards were vortexed in 6, 9, 12 mol L⁻¹ (commonly used in polysaccharide pretreatment), and 13.5 mol L⁻¹ (used in the PSA method) H₂SO₄ for 15 s. The resulting hydrolysates were loaded into a 96-well microplate (655101; Greiner). The reagent blank is H₂SO₄ in the same molarity as in the hydrolysis step (all 250 μ L, two replicates). UV/VIS spectra were recorded by Varian LUX microplate reader (Thermo Fisher Scientific) from 200 to 800 nm with 2 nm steps. The UV spectra indicate that sulfuric acid concentrations used in hydrolysis should not exceed 9 mol L⁻¹ to prevent excessive dehydration.

Glucose, fructose, xylose, galactose, fucose, and galacturonic acid were mixed with 1.6, 3, 6, and 9 mol L⁻¹ H₂SO₄ respectively and immediately vortexed for 15 s. The mixtures were incubated in a water bath at 90°C (used in the PSA method) or the boiling point (commonly used in other hydrolysis methods). Triplicates were removed from water bath every 20 min. Hydrolysates were alkalized and then analyzed by the TPTZ method.

Polysaccharide hydrolysis: Duration and pretreatment

To determine the optimal acid hydrolysis duration for common polysaccharides, the water-soluble polysaccharides laminarin, alginate, and water-insoluble cellulose, amylose, pectin, and chitin, and the monosaccharides glucose and fructose were hydrolyzed in 1.6 mol L⁻¹ H₂SO₄ at 90°C. To determine whether hydrolysis with an additional acid pretreatment could yield higher recoveries from polysaccharides we repeated the experiment with a 9 mol L⁻¹ H₂SO₄ pretreatment. Five hundred microliters of 18 mol L⁻¹ H₂SO₄ was added to 500 μ L polysaccharide standards, and then immediately vortexed for 15 or 30 s (final molarity of H₂SO₄ in this pretreatment was 9 mol L⁻¹), then another 4.5 mL of Milli-Q water was added to dilute H₂SO₄ into 1.6 mol L⁻¹ without further vortexing. The tubes were placed in a 90°C water bath. Triplicates were removed from water bath at 20-min intervals during the first hour and then at 60-min intervals from 1 to

3 h. Hydrolysates were alkalized and then analyzed using the TPTZ method.

Other hydrolysis methods

We pretreated glucose by 12 mol L⁻¹ H₂SO₄ and then diluted to 1.2 mol L⁻¹ H₂SO₄ for 3 h at 100°C (Pakulski and Benner 1992). We evaluated the hydrolysis of oligo- and polysaccharide standards by using 0.1 mol L⁻¹ HCl at 100°C for 20 h (Myklestad et al. 1997) and 1.2 mol L⁻¹ H₂SO₄ for 3 h at 100°C without pretreatment (Hung et al. 2003). After hydrolysis, hydrolysate was alkalized and then measured by the TPTZ method. We also quantified monosaccharide, oligo- and polysaccharide standards and microalgae samples using the PSA method (Laurens et al. 2012).

Optimized hydrolysis procedure

Five hundred microliters of 18 mol L⁻¹ H₂SO₄ was added into each centrifuge tube with carbohydrate standards or filters with phytoplankton samples and then immediately vortexed for 15 s. Another 4.5 mL of Milli-Q water was added without further vortex. The tubes were placed in a 90°C water bath for 3 h.

Influence of hydrolysate pH on TPTZ method

We tested how the pH of the hydrolysate affected the measurement of reducing groups from dehydrated and non-dehydrated glucose by the TPTZ method. Hydrolysate aliquots were transferred into amber vials followed by the addition of 12 mol L⁻¹ NaOH and topped up to 1 mL by Milli-Q water. The ratio between [H⁺] from hydrolysate and [OH⁻] from NaOH was 1.13, 1, 0.9, and 0.82.

The results led to our recommendation that hydrolysate needs to be alkalized for a complete measurement of carbohydrate in the TPTZ method. To alkalize the hydrolysate of carbohydrate standards or phytoplankton samples, the necessary volume of 12 mol L⁻¹ NaOH was added to achieve a ratio of [H⁺] from the hydrolysate to [OH⁻] from NaOH of 0.82. The resulting volume of alkalized hydrolysate was adjusted to 1 mL by adding Milli-Q water.

TPTZ analysis

Preparation of reagents in the TPTZ method followed Avigad (1975) and Myklestad et al. (1997). Reagent solutions were stored at room temperature. The alkaline solution for Reagent A was a mixture of 400 mg NaOH and 20 g Na₂CO₃ per liter of solution in Milli-Q water. Reagent A was made by dissolving 23 mg K₃[Fe(CN)₆] in 100 mL of the alkaline solution. The acetate solution for reagent B was made from a mixture of 164 g sodium acetate (anhydrous), 42 g citric acid, and 300 g acetic acid per liter of solution in Milli-Q water. Reagent B was prepared by dissolving FeCl₃·6H₂O in the acetate solution for a final concentration of 54 mg per 100 mL. The acetic acid solution for reagent C was a solution of 3 mol L⁻¹ acetic

acid in Milli-Q water (180 g L⁻¹). Reagent C was prepared by dissolving 78 mg TPTZ in 100 mL of the acetic acid solution.

One milliliter of reagent A was added into the alkalized hydrolysate. After a 10-min incubation in a boiling water bath, 1 mL of reagent B and 2 mL of reagent C were added, and the mixture was vortexed and continuously shaken at room temperature for 30 min. Then 250 μL of the resulting mixture was dispensed into duplicate wells of a 96-well microplate (655101; Greiner), column by column. Each column was covered to avoid light exposure as soon as all eight wells were loaded. After a 5 s shake, the absorbance at 595 nm was measured using a microplate reader (Varioskan LUX; Thermo Fisher Scientific) at room temperature, with a path length of 5 mm.

Data analysis

The TPTZ standard curve is a regression of the absorbance of the TPTZ-Fe²⁺ measured at 595 nm in a microplate reader at room temperature (corrected by the absorbance from the reagent blank) as a function of the carbon concentration (μg C mL⁻¹). The limit of detection (LOD) or quantitation (LOQ) was calculated as $k \times S_y / S$, where S_y is the standard deviation of the absorbance from reagent blank, S is the slope of the standard curve, and k is a constant equal to 3 for LOD and 10 for LOQ recommended by IUPAC (Jochum et al. 1981).

The measured carbon (C_m , μg C mL⁻¹) in a carbohydrate standard is quantified equivalent to a hydrolyzed glucose standard under the same hydrolysis conditions with the formula:

$$C_m = (A - A_{\text{blank}} - b_{\text{HGlu}}) / a_{\text{HGlu}}, \quad (1)$$

where A is the absorbance from the carbohydrate standard in TPTZ method, A_{blank} is the absorbance from reagent blank, b_{HGlu} and a_{HGlu} is the intercept and slope of the standard curve of hydrolyzed glucose, respectively.

The actual carbon concentration in a carbohydrate standard solution (C_a , μg C mL⁻¹) is calculated with the formula:

$$C_a = \text{Conc}(12.01 N / \text{MW})P, \quad (2)$$

where Conc is the actual concentration of the carbohydrate standard (μg mL⁻¹), N is the number of carbon atoms in the molecular formula of the carbohydrate standard compound, MW is the molecular weight of the standard compound, and P is the purity of the standard.

The recovery of carbon in a carbohydrate standard (R_C) is calculated with the formula:

$$R_C = C_m / C_a. \quad (3)$$

The colorimetric signal produced by the TPTZ assay is proportional to the number of aldehyde and hydroxyl groups, collectively referred to as reducing groups. The total number of reducing groups varies depending on the specific

monosaccharide and its configuration. Dehydration occurring during hydrolysis can alter the number of reducing groups present in the analyte. Moreover, the pH of the analyte affects the deprotonation of reducing groups, thereby influencing the reducing activity of the analyte, and resulting in variations in recovery. The observed number of reducing groups per sugar is

$$n = 6 \times R_C, \quad (4)$$

where R_C is the recovery of carbohydrate, and six denotes the number of reducing groups in acyclic glucose.

Data analyses were performed using the statistical software R version 4.1.2 and RStudio version 4.1.2. Error estimates provided in figures, results, and the discussion were one standard deviation from three replicates, unless otherwise noted. Chemical structures were drawn by ACD/ChemSketch.

Assessment

We investigated many variations on the hydrolysis and alkalization steps in the TPTZ protocol. We present key findings and a recommended optimized procedure for quantifying bulk carbohydrate. We found that variations in hydrolysis and alkalization conditions affected the detection of glucose and the overall sensitivity of the TPTZ assay. Subsequently, we explored a variety of hydrolysis steps on mono-, oligo-, and polysaccharide standards, before applying the optimized method to biological samples.

Hydrolysis conditions can dehydrate glucose

High concentrations of Brønsted acids, such as HCl and H₂SO₄, promote the acid-catalyzed dehydration (Mellmer et al. 2019) of glucose into 5-(hydroxymethyl) furfural (HMF; Itagaki 1994; Fig. 1), changing its absorption spectrum in the UV region. UV spectra for glucose illustrate the influence of hydrolysis conditions on glucose dehydration (Fig. 2). A 15 s vortex in 13.5 mol L⁻¹ H₂SO₄ resulted in a prominent absorbance at approximately 320 nm, while the 12 mol L⁻¹ H₂SO₄ condition showed a moderate absorbance around 300 nm. A weak absorbance was observed in glucose vortexed in 9 mol L⁻¹ H₂SO₄, and glucose vortexed for 15 s in 6 mol L⁻¹ H₂SO₄ displayed UV spectra similar to those of unhydrolyzed glucose, remaining transparent. The peaks in UV spectra indicate the formation of polymerized HMF and other derivatives, such as

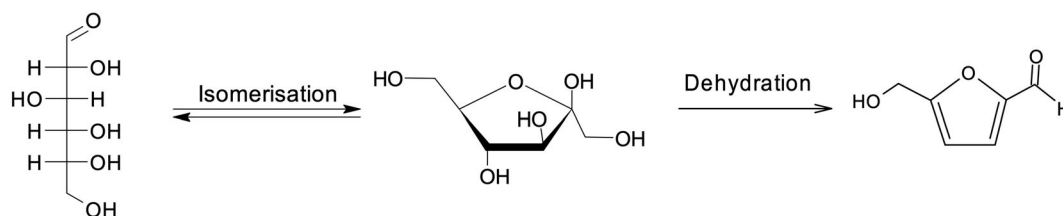


Fig. 1. Scheme of glucose dehydration in H₂SO₄.

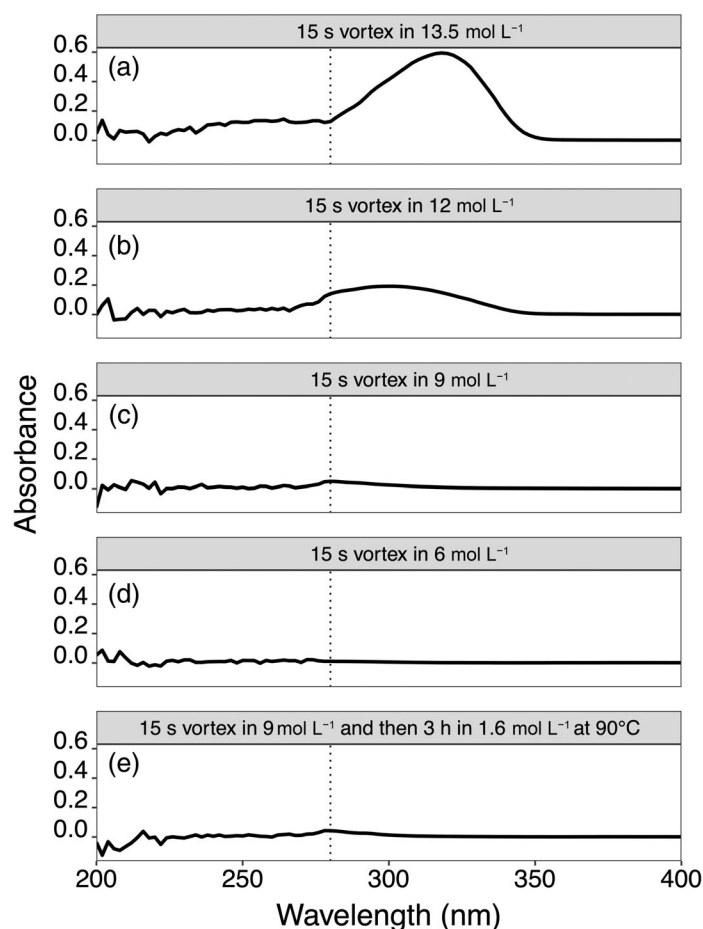


Fig. 2. UV spectra of glucose depicting distinctive absorbance patterns. Hydrolysis conditions are reported in the title of each panel.

5,5'-(oxydimethylene)-di-2-furaldehyde (Gandini 1997; Wang et al. 2018). This dehydration potentially occurred in some published protocols, such as those involving pretreatment with 12 mol L⁻¹ H₂SO₄ at room temperature for 2 h, followed by incubation at 100°C for 3 h in 1.2 mol L⁻¹ H₂SO₄, as described by Pakulski and Benner (1992). Since glucose remained transparent in the UV region after a 15 s vortex in 9 and 6 mol L⁻¹ sulfuric acid (Fig. 2c,d), we recommend using 9 mol L⁻¹ sulfuric acid to pretreat carbohydrate samples. Our recommended optimized hydrolysis step (15 s vortex in 9 mol L⁻¹ H₂SO₄ followed by a 3 h hydrolysis at 90°C in 1.6 mol L⁻¹ H₂SO₄) had no

discernible impact on the glucose structure (Fig. 2e). The faint absorbance at 280 nm in Fig. 2c,e possibly arises from furanose with an undehydrated aldehyde (Sarazin et al. 2011) rather than dehydration.

The importance of alkalizing the hydrolysate

The pH of the analyte alters both carbohydrate chemistry and TPTZ color development. Glucose, pretreated with $9 \text{ mol L}^{-1} \text{ H}_2\text{SO}_4$ and hydrolyzed by $1.6 \text{ mol L}^{-1} \text{ H}_2\text{SO}_4$ at 90°C for 3 h (the optimized hydrolysis) might exist in acyclic, cyclic or a combination of both forms, resulting in an expected five to six reducing groups. We find the measured number of reducing groups varied from 5.6 in acidic solution, 5.4 in a neutralized solution, 5.1 in slightly alkalized solution, to 5 in a more alkalized solution (Fig. 3, black diamonds). Acyclic D-glucose solution has a pH of around 8 at very low concentrations, decreasing to acidic values with increased glucose concentration (Feng et al. 2013). These results indicate that acyclic D-glucose is more acidic than cyclic D-glucose (D-glucopyranose) and can fully deprotonate even in slightly acidic solutions. The alkalized medium stabilizes glucose in a complete cyclic structure, consistently providing five reducing groups from glucose.

The sensitivity of the assay increased with progressively large amounts of added hydroxide, leading to enhanced color development across a range of carbon concentrations. We observed a linear relationship ($R^2 = 0.9998$) between blank corrected absorbance at 595 nm for TPTZ- Fe^{2+} and the concentration of carbon ($\mu\text{g C mL}^{-1}$) from glucose hydrolyzed in our optimized hydrolysis method (Fig. 4). The absolute absorbance from the reagent blank at 595 nm was 0.05. The low detection limit (L-LOD) and low quantitation limit (L-LOQ) were calculated as 5 and 16 ng C mL^{-1} , respectively. The high detection limit (H-LOD) was $10 \mu\text{g C mL}^{-1}$. Alkalization of the hydrolysate resulted in a 29% increase in the molar absorptivity (ϵ) of TPTZ- Fe^{2+} compared to the value reported by Myklestad et al. (1997) using hydrolysate

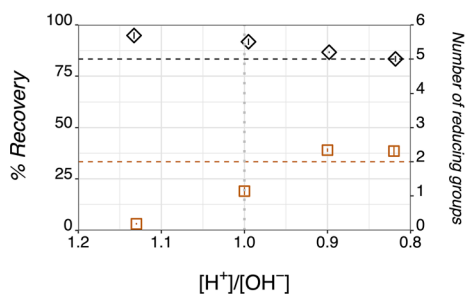


Fig. 3. Dehydrated glucose in $13.5 \text{ mol L}^{-1} \text{ H}_2\text{SO}_4$ (red squares) and glucose pretreated by $9 \text{ mol L}^{-1} \text{ H}_2\text{SO}_4$ followed by hydrolysis in $1.6 \text{ mol L}^{-1} \text{ H}_2\text{SO}_4$ at 90°C for 3 h (black diamonds) measured by TPTZ after the hydrolysate was treated with $12 \text{ mol L}^{-1} \text{ NaOH}$. Ratios of $[\text{H}^+]$ from the hydrolysate to $[\text{OH}^-]$ from $12 \text{ mol L}^{-1} \text{ NaOH}$ were 1.13, 1.00 (vertical dashed line), 0.90, and 0.82. The expected number of reducing groups for each treatment is depicted with a horizontal dashed line.

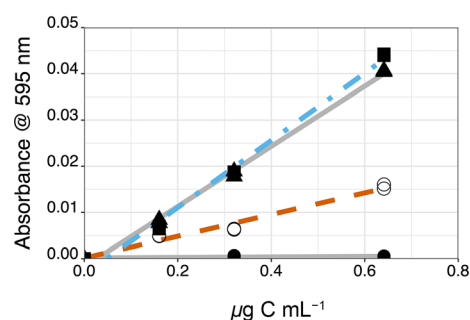


Fig. 4. Colorimetric response of TPTZ- Fe^{2+} complex depends on the amount of $12 \text{ mol L}^{-1} \text{ NaOH}$ added. The ratio $[\text{H}^+]/[\text{OH}^-]$ is indicated by the symbol: 1.13 (solid circles), 1.00 (circles), 0.90 (solid triangles), and 0.82 (solid squares). Lines are from linear regression (four treatments, two replicates). The blue dot-dashed line denotes the optimized alkalization treatment while the red dashed line marks the traditionally used neutralization.

neutralization ($3899 \pm 56 \text{ L mol}^{-1} \text{ cm}^{-1}$, pathlength 5 mm vs. $\sim 3030 \text{ L mol}^{-1} \text{ cm}^{-1}$, pathlength 20 mm). The highest sensitivity (slope of absorbance corrected by the blank vs. carbon concentration) for detecting hydrolyzed glucose by TPTZ was obtained from an alkalized hydrolysate (solid squares in Fig. 4), in which the ratio of $[\text{H}^+]$ from hydrolysate to $[\text{OH}^-]$ from $12 \text{ mol L}^{-1} \text{ NaOH}$ was 0.82. The excess $[\text{OH}^-]$ beyond what was needed to neutralize the solution gave a final pH 13.68, which was higher than the pH of ferricyanide reagent A (measured pH 11.24 at 20°C).

The apparent loss of sugar observed during different neutralization procedures (Panagiotopoulos and Sempéré 2005) likely arises from the incomplete deprotonation of reducing groups. This incomplete deprotonation diminishes the molar absorptivity of the colored complex and therefore carbohydrate recovery. The deprotonation of a monosaccharide for reducing ferricyanide depends on pH and is expected to occur when the redox potential of $\text{R-H-e} \leftrightarrow \text{R}\cdot + \text{H}^+$ falls below that of the pH-independent ferricyanide-ferrocyanide system (Speakman and Waters 1955). A fully dehydrated glucose (HMF) with a pK_a value of about 12.82 (Rizelio et al. 2012) would deprotonate its hydroxyl and aldehyde groups only at pH levels ≥ 12.82 . We observed the expected two reducing groups from fully alkalized hydrolysates with an $[\text{H}^+]/[\text{OH}^-]$ ratio of 0.90 or 0.82 (Fig. 3, red squares), while the neutralized analyte yielded only one reducing group. Consequently, the recovery of dehydrated glucose (HMF) in a neutralized hydrolysate is only 50% in the TPTZ analysis without alkalization. This clarifies why mannuronic acid shows a 51% recovery and galacturonic acid exhibits a 71% recovery in the TPTZ method without alkalization of the monosaccharide solution (Myklestad et al. 1997). Both uronic acids share a similar structure, potentially resulting in closer proton affinities compared to glucuronic acid. We assume the presence of a carboxyl group may contribute to a higher pK_a value. The acidic environment from the uronic acid solution may lead to

Table 1. Influence of hydrolysis conditions on absorbance of hydrolyzed glucose relative to the absorbance of unhydrolyzed glucose measured by the TPTZ method.

Pretreatment	Acid in hydrolysis	Temperature (°C)	Duration	Absorbance relative to unhydrolyzed glucose (%)
No	0.1 mol L ⁻¹ HCl	100	20 h	63
No	1.2 mol L ⁻¹ H ₂ SO ₄	ATHV	15 s	84
No	1.2 mol L ⁻¹ H ₂ SO ₄	100	3 h	89
12 mol L ⁻¹ H ₂ SO ₄	1.2 mol L ⁻¹ H ₂ SO ₄	100	3 h	75
No	1.6 mol L ⁻¹ H ₂ SO ₄	AT	15 s	85
No	1.6 mol L ⁻¹ H ₂ SO ₄	90	3 h	83
9 mol L ⁻¹ H ₂ SO ₄	1.6 mol L ⁻¹ H ₂ SO ₄	90	3 h	83
No	13.5 mol L ⁻¹ H ₂ SO ₄	ATHV	15 s	33

ATHV, ambient temperature with heating due to vortexing.

incomplete deprotonation of all reducing groups, causing lower recovery than from other monosaccharides.

We recommend alkalinizing the hydrolysate (so that the ratio of [H⁺] from the hydrolysate to [OH⁻] from the 12 mol L⁻¹ NaOH is equal to 0.82) for two main reasons: (1) this pH condition promotes the presence of D-glucopyranose with five reducing groups, ensuring consistent carbon recovery; (2) it facilitates the complete deprotonation of all carbohydrate reducing groups, allowing maximum reduction of ferricyanide to ferrocyanide, thus generating the maximum TPTZ-Fe²⁺ complex for the highest carbohydrate recovery.

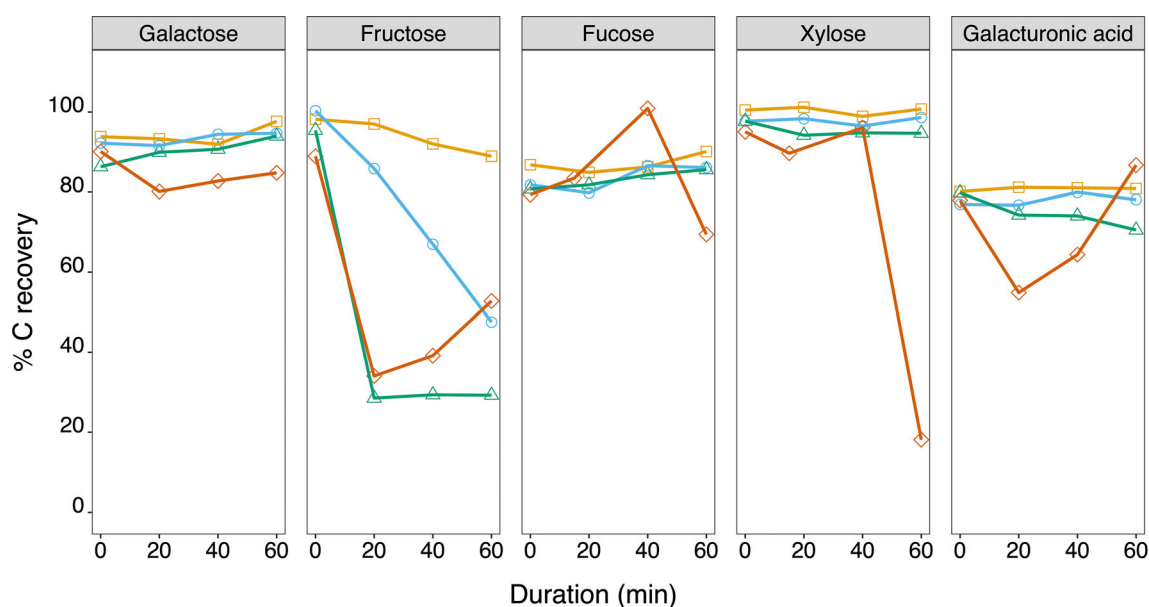
Effect of hydrolysis conditions on glucose recovery

We hydrolyzed the glucose standard using a range of conditions, varying the use of a pretreatment, acid and

concentration, temperature, and duration. The hydrolysate was alkalinized before measurement using the TPTZ method. The observed absorbance, relative to unhydrolyzed glucose, varied from 33% to 89% (Table 1), with the lowest from glucose vortexed in 13.5 mol L⁻¹ H₂SO₄ and the highest from glucose hydrolyzed in 1.2 mol L⁻¹ H₂SO₄ at 100°C for 3 h, respectively.

Effect of hydrolysis conditions on monosaccharide recovery

A 1.6 mol L⁻¹ H₂SO₄ hydrolysis demonstrated superior recovery compared to 3, 6, or 9 mol L⁻¹ H₂SO₄ across a set of representative monosaccharides (galactose, fructose, fucose, xylose, and galacturonic acid) which are subunits of aldohexose, ketohexose, deoxysugar, aldopentose, and uronic

**Fig. 5.** Time course of carbon recovery of galactose, fructose, fucose, xylose, and galacturonic acid equivalent to glucose using different concentrations of H₂SO₄ in a 90°C water bath: 1.6 mol L⁻¹ (orange squares), 3 mol L⁻¹ (blue circles), 6 mol L⁻¹ (green triangles), 9 mol L⁻¹ (red diamonds).

acid (Fig. 5). The acid concentration during the initial 15 s vortex had limited impact on the recovery of individual monosaccharides, except for a 10% decrease in fructose recovery with 9 mol L^{-1} compared to 1.6 mol L^{-1} H_2SO_4 . During the initial hour of hydrolysis in 1.6 mol L^{-1} H_2SO_4 at 90°C , the number of reducing groups remained stable: approximately six for glucose, fructose, fucose, galactose, and xylose, while galacturonic acid displayed four reducing groups (Fig. 6). Galacturonic acid had the lowest recovery (80%) among the assessed monosaccharides, but its recovery, relative to glucose, increased after hydrolysis in 9 mol L^{-1} H_2SO_4 . The decrease in the number of reducing groups in galacturonic acid is consistent with the substitution of one hydroxyl group by a carboxylic acid in uronic acid. Consequently, the anticipated maximum recovery from uronic acid equivalent to glucose is approximately 80%, given its four reducing groups compared to the five in D-glucopyranose.

Fructose exhibited higher sensitivity to both H_2SO_4 concentration and temperature increase, compared to the other monosaccharides (Figs. 5–7). Fructose recovery declined by 3% in 1.6 mol L^{-1} H_2SO_4 , 17% in 3 mol L^{-1} H_2SO_4 , 67% in 6 mol L^{-1} H_2SO_4 , and 55% in 9 mol L^{-1} H_2SO_4 within the initial 20 min. After 1 h in 3 mol L^{-1} H_2SO_4 , the graduate dehydration of fructose resulted in the removal of three reducing groups, reducing its count from 5.4 to 2.5 (Fig. 6) and its

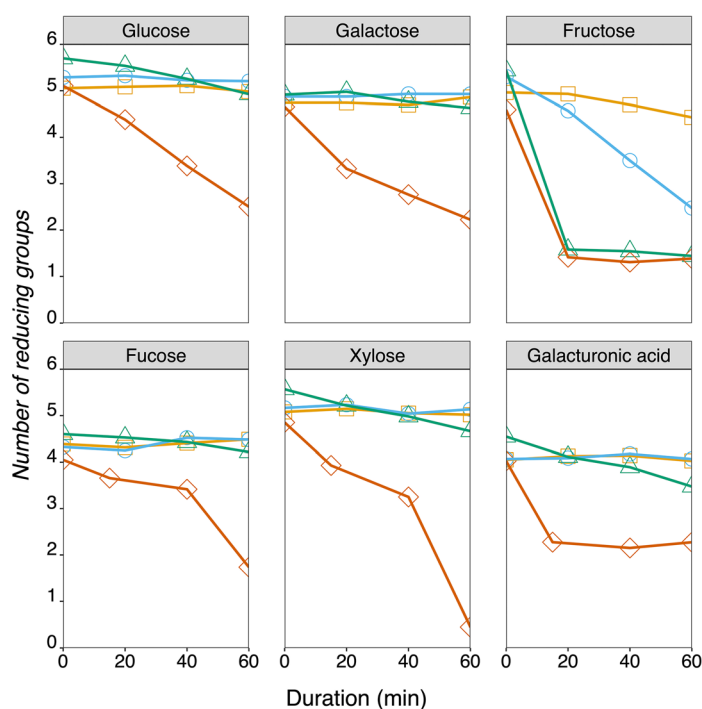


Fig. 6. The effect of hydrolysis conditions on the number of reducing groups as a function of time for glucose, galactose, fructose, fucose, xylose, and galacturonic acid. Hydrolysis at 90°C and H_2SO_4 molarity: 1.6 mol L^{-1} (orange squares), 3 mol L^{-1} (blue circles), 6 mol L^{-1} (green triangles), 9 mol L^{-1} (red diamonds).

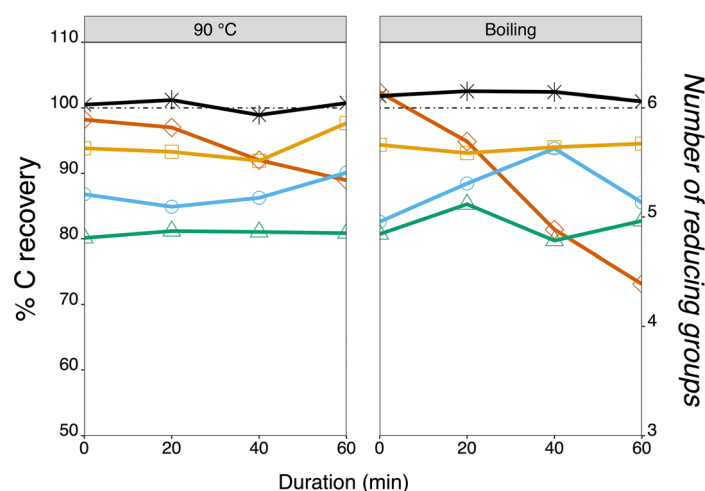


Fig. 7. Time course of carbon recovery of fructose (red diamonds), fucose (blue circles), galactose (orange squares), galacturonic acid (green triangles), and xylose (black asterisks) equivalent to glucose under the same conditions in 1.6 mol L^{-1} H_2SO_4 at 90°C or boiling water bath (100°C).

recovery from 100% to 48% (Fig. 5). Extended hydrolysis (up to 3 h) in 1.6 mol L^{-1} H_2SO_4 at 90°C did not cause further dehydration of glucose, but the number of reducing groups from fructose decreased to 2, leading to only 30% recovery equivalent to glucose (Fig. 8), likely due to fructose dehydration to levulinic acid (Mulder 1840). At 100°C , the recovery of fructose decreased by approximately 15% compared to 90°C in 1.6 mol L^{-1} H_2SO_4 after 1 h (Fig. 7). Feng et al. (2013) noted that fructose exhibits stronger acidic properties compared to glucose, which could contribute to its self-catalyzed dehydration reactions. Selvendran et al. (1979) and Borch and Kirchman (1997) noted a decrease in monosaccharide recovery with prolonged hydrolysis, potentially caused by the loss of reducing groups. This heightened susceptibility of fructose to dehydration might elucidate why pentoses are more prone to partial or complete loss during hydrolysis compared to hexoses (Borch and Kirchman 1997).

Our results show how hydrolysis conditions (duration, temperature, and acid concentration) affect recovery of monosaccharides and the number of reducing groups. We find that a 9 mol L^{-1} H_2SO_4 pretreatment for 15 s followed by a 1.6 mol L^{-1} H_2SO_4 hydrolysis for 3 h at 90°C is a good compromise for C recovery from diverse carbohydrates. Hydrolysis in 1.2 or 1.6 mol L^{-1} H_2SO_4 with no pretreatment at a range of temperatures and incubation times resulted in significantly less loss in molar absorptivity from glucose (relative to non-hydrolyzed glucose) than the 0.1 mol L^{-1} HCl hydrolysis at 100°C for 20 h (Myklestad et al. 1997), which reduced the absorbance of glucose to 63% relative to unhydrolyzed glucose (Table 1). Long duration hydrolysis with diluted HCl at 100°C leads to low recovery of glucose. Similarly, a 15 s 13.5 mol L^{-1} H_2SO_4 treatment reduced glucose absorbance to 33% relative to unhydrolyzed glucose, but a 15 s 9 mol L^{-1} H_2SO_4

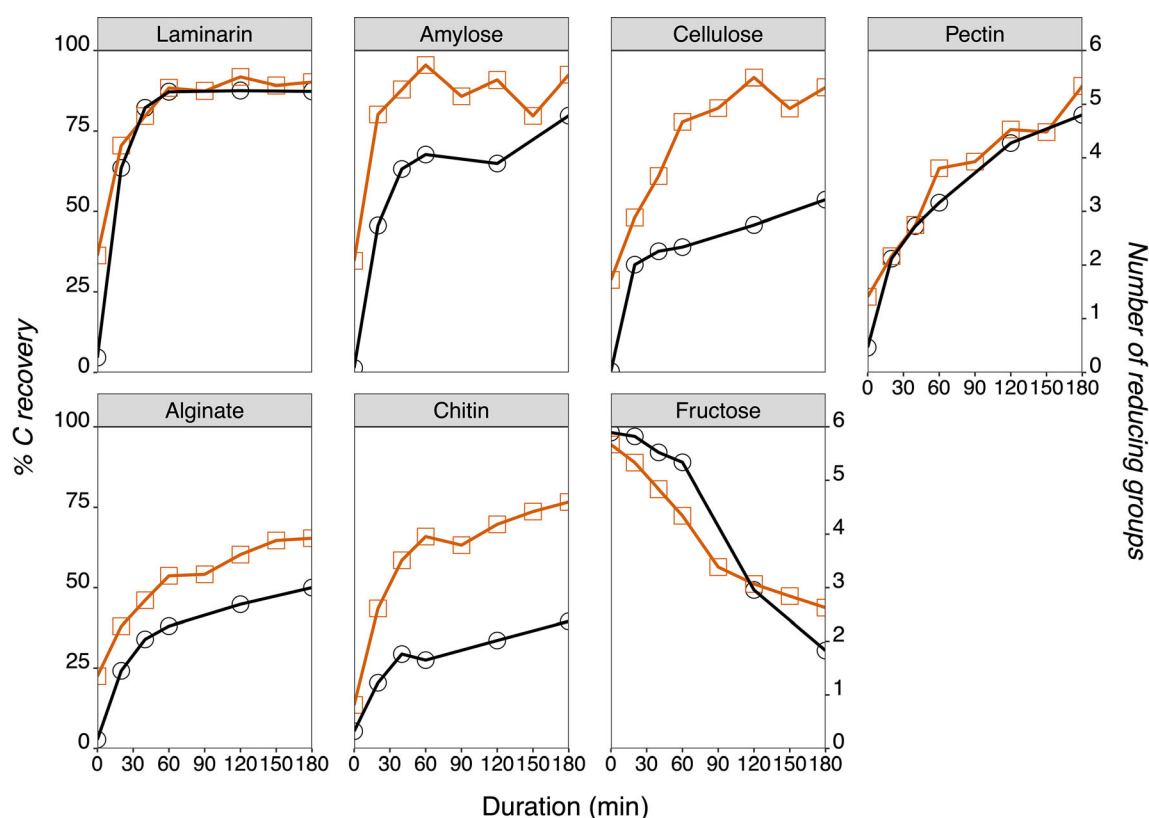


Fig. 8. Comparison of the carbon recovery of laminarin, amylose, cellulose, pectin, alginate, chitin, and fructose hydrolyzed in $1.6 \text{ mol L}^{-1} \text{ H}_2\text{SO}_4$ at 90°C with (red) or without (black) pretreatment by $9 \text{ mol L}^{-1} \text{ H}_2\text{SO}_4$. The monosaccharide fructose is included due to its sensitivity to hydrolysis duration, providing insights into the impact of polysaccharides hydrolysis on overall carbohydrate recovery.

pretreatment followed by a $1.6 \text{ mol L}^{-1} \text{ H}_2\text{SO}_4$ hydrolysis at 90°C for 3 h only led to moderate absorbance loss. The UV spectra confirm the highest level of dehydration in the 15 s $13.5 \text{ mol L}^{-1} \text{ H}_2\text{SO}_4$ hydrolysis treatment, a lower level of dehydration at 12 mol L^{-1} , and undetectable levels of dehydration with 15 s 9 and 6 mol L^{-1} treatment and with the two-step hydrolysis (pretreatment by $9 \text{ mol L}^{-1} \text{ H}_2\text{SO}_4$ and then incubation at 90°C in $1.6 \text{ mol L}^{-1} \text{ H}_2\text{SO}_4$ for 3 h) (Fig. 2).

Contrasting effects of hydrolysis conditions on glucose compared to other monosaccharides results in complex patterns of monosaccharide recovery since recovery is quantified relative to glucose. A 15 s hydrolysis with $9 \text{ mol L}^{-1} \text{ H}_2\text{SO}_4$ did not induce dehydration in glucose, a finding supported by UV spectra (Fig. 2c). The brief 15 s vortex of monosaccharides in $9 \text{ mol L}^{-1} \text{ H}_2\text{SO}_4$ resulted in recoveries ranging from 80% to 90% (Fig. 5); however, prolonged exposure showed signs of dehydration across all monosaccharides with time (Fig. 6). Under 1 h hydrolysis in $9 \text{ mol L}^{-1} \text{ H}_2\text{SO}_4$ at 90°C , glucose lost an average of 2.5 hydroxyl groups, while galactose, galacturonic acid, fucose, fructose, and xylose lost 2.7, 2.7, 3.3, 3.7, and 4.6 hydroxyl groups, respectively. Different monosaccharides underwent distinct dehydration reactions: uronic acid dehydrates to 2-furonic acid (Rosenau et al. 2017),

glucose, fucose, and galactose to furfural, and fructose and xylose to levulinic acid (Hu et al. 2017). This resulted in varying recovery rates: 80% for galacturonic acid and galactose, 65% for fucose, 50% for fructose, and 15% for xylose (Fig. 5). Swain and Bratt (1972) reported increased recovery rates of glucose and mannose by 20% and 10%, respectively, after pretreatment of sediments in cold concentrated H_2SO_4 . In contrast, Borch and Kirchman (1997) observed decreased recovery rates for galactose, fucose and rhamnose following strong acid pretreatment. Understanding the differing dehydration tendencies of various monosaccharides helps clarify how recovery rates can fluctuate with alterations in hydrolysis conditions. In our optimized hydrolysis, we recommend a $9 \text{ mol L}^{-1} \text{ H}_2\text{SO}_4$ pretreatment for 15 s.

Impact of pretreatment on polysaccharide recovery

Compared to the single-step hydrolysis, the pretreatment step with $9 \text{ mol L}^{-1} \text{ H}_2\text{SO}_4$ enhanced the recovery of tested polysaccharides, including alginate (+15%), amylose (+13%), cellulose (+35%), pectin (+9%), and chitin (+37%) (Fig. 8). The recovery of laminarin ($90\% \pm 4\%$) showed only a marginal improvement, with a 3% increase compared to no pretreatment. This result aligns with the recovery reported by

Pakulski and Benner (1992), who used a $12 \text{ mol L}^{-1} \text{ H}_2\text{SO}_4$ pretreatment followed by a 3 h hydrolysis in $1.2 \text{ mol L}^{-1} \text{ H}_2\text{SO}_4$ at 100°C . No significant differences in carbohydrate recovery were observed in most cases between 15 and 30 s of pretreatment (Fig. 9). The recovery of chitin remained unchanged after the vortex step but increased by 15% following a 1-h incubation when using a 15-s pretreatment compared to a 30-s pretreatment.

The $9 \text{ mol L}^{-1} \text{ H}_2\text{SO}_4$ pretreatment increased the water solubility of various polysaccharides, preventing precipitation in the two-step hydrolysis of amylose, cellulose, chitin, and pectin. During the single-step hydrolysis, precipitates were evident in the amylose, cellulose, chitin, and pectin hydrolysate, but absent following pretreatment. The improvement in recovery suggests that the pretreatment expedited the cleavage of glycosidic bonds. The varying recovery rates across polysaccharides following pretreatment reflect their diverse compositions and bond structures. For instance, laminarin, composed of glucose units linked by $\beta(1 \rightarrow 3)$ and $\beta(1 \rightarrow 6)$ bonds showed a recovery limit of approximately 90% due to the competition between the hydrolysis of the glycosidic linkage and the protonation of glycosidic O atom (Kamerling and

Gerwig 2007; Fig. 5). In contrast, amylose, comprising glucose units connected via $\alpha(1 \rightarrow 4)$ glycosidic bonds, displayed an initial recovery acceleration to 95% in 1 h but then remained constant during secondary reactions in both the amorphous and crystalline region (Wang and Copeland 2015). Cellulose, with $\beta(1 \rightarrow 4)$ glycosidic bonds between its glucose units, exhibited an increased initial solubility with pretreatment, allowing greater acid access. However, its hydrolysis rate eventually stabilized, resulting in a final recovery of $89\% \pm 2\%$. Our method's lower H_2SO_4 molarity (1.6 mol L^{-1}) limited cellulose recovery compared to the PSA method ($104\% \pm 2\%$; Table 3).

The recovery of polysaccharides like alginate, pectin, or chitin is partially due to the number of reducing groups in uronic acid and amino sugar (four to five vs. five to six reducing groups in glucose), as well as the hydrolysis duration and acid concentration. Considering fructose's recovery decrease to 50% in the 3 h two-step hydrolysis (Fig. 8), extending hydrolysis is only recommended for samples dominated by polysaccharides like alginate and cellulose. Complete recovery of alginate during hydrolysis might be achieved with stronger acid concentration; however, this approach must be carefully considered due to potential dehydration and chromophore

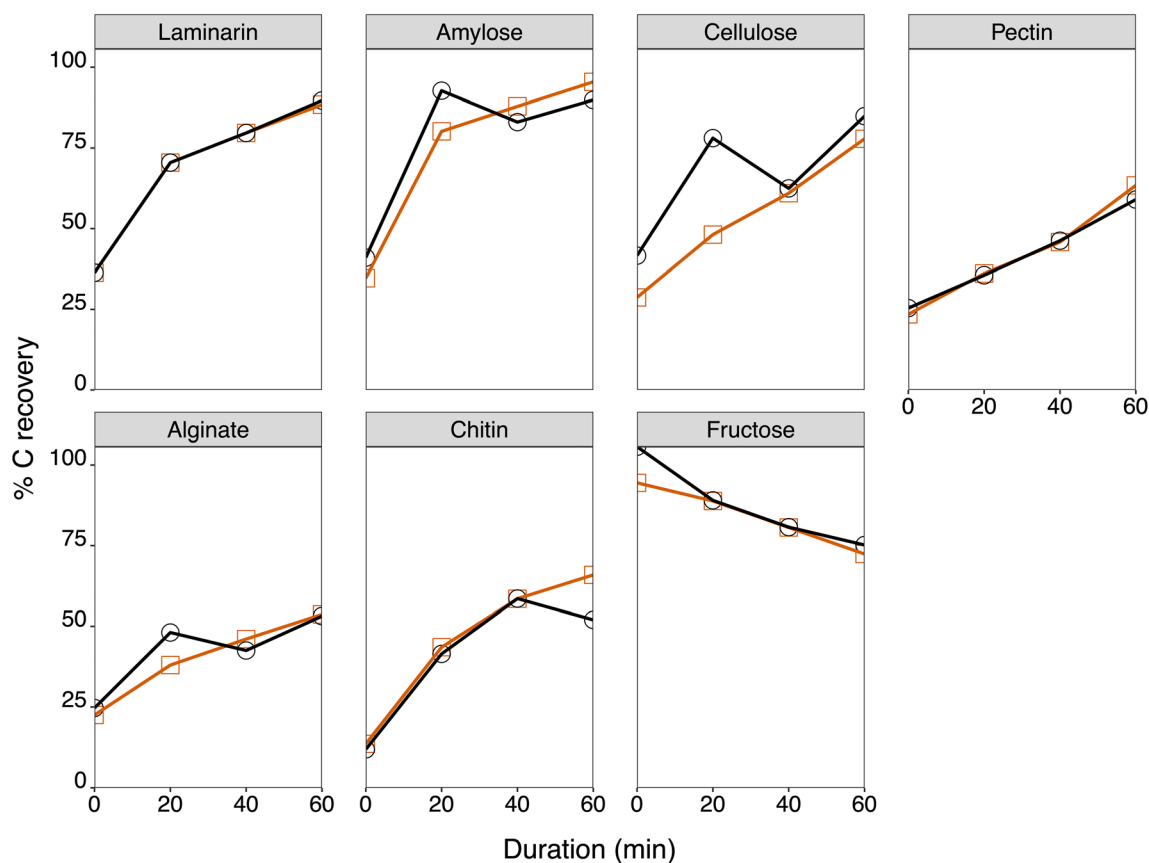


Fig. 9. Comparison of the carbon recovery for laminarin, amylose, cellulose, pectin, alginate, chitin, and fructose vortexed in $9 \text{ mol L}^{-1} \text{ H}_2\text{SO}_4$ for 15 s (red) or 30 s (black), followed by 1 h hydrolysis in $1.6 \text{ mol L}^{-1} \text{ H}_2\text{SO}_4$ at 90°C . The monosaccharide fructose is included due to its sensitivity to hydrolysis duration, providing insights into the impact of polysaccharides hydrolysis on overall carbohydrate recovery.

formation (Rosenau et al. 2017). In addition, acid breakdown may be protected by the glycan structure in alginate (Haug and Larsen 1965), further complicating the optimization of the hydrolysis process.

Recovery of carbohydrate standards

Twelve monosaccharide standards were selected to evaluate our optimized method, encompassing common aldohexoses, deoxysugars, ketohexoses, aldopentoses, uronic acids, and amino sugars found in the marine environment. Our assessment compared recovery across three methods: (1) our optimized hydrolysis method followed by alkalization of hydrolysate and subsequent TPTZ method (TPTZ-op-H₂SO₄), (2) the PSA method, and (3) the TPTZ method with neither hydrolysis nor alkalization of sugar solution (as reported by Myklestad et al. 1997). The optimized hydrolysis method achieved a mean recovery of 94% from these standards, equivalent to glucose, except for fructose (Table 2). The new TPTZ-op-H₂SO₄ method significantly enhances reproducibility and recovery compared to other methods. The monosaccharides rhamnose and arabinose exhibited approximately 20% higher recovery with our optimized hydrolysis and alkalization of hydrolysate compared to the method reported by Myklestad et al. (1997), which lacks both hydrolysis and alkalization steps before the TPTZ reaction. Fructose recovery was greatly reduced relative to Myklestad's method to only 44% ± 5%.

Our optimized method achieved greater recovery for most deoxysugars, aldopentoses, and uronic acids tested relative to the results reported by Myklestad et al. (1997). The PSA method exhibited highly variable recovery from monosaccharides, overestimating fucose (118%) and fructose (162%), while underestimating many other monosaccharide standards

(21–72%) and failed to detect *N*-acetyl-D-glucosamine (Table 2).

Oligo- and polysaccharides, such as sucrose, raffinose, laminarin, amylose, cellulose, alginate, pectin, and chitin, were subjected to three hydrolysis methods for analysis: (1) our optimized hydrolysis method (TPTZ-op-H₂SO₄), (2) hydrolysis in 0.1 mol L⁻¹ HCl for 20 h at 100°C (TPTZ-HCl; Myklestad et al. 1997), and (3) hydrolysis in 1.2 mol L⁻¹ H₂SO₄ for 3 h at 100°C (TPTZ-H₂SO₄; Hung et al. 2003). Each hydrolysis method was followed by alkalization of the hydrolysate and measurement using the TPTZ method. The hydrolysis with 12 mol L⁻¹ H₂SO₄ pretreatment followed by 1.2 mol L⁻¹ H₂SO₄ for 3 h at 100°C (Pakulski and Benner 1992) was excluded from the comparison due to significant dehydration, as confirmed by UV spectra analysis (Fig. 2b). The PSA method was included for comparison purposes.

For glucose-based compounds, our optimized hydrolysis displayed an average of 85% recovery, surpassing TPTZ-HCl and TPTZ-H₂SO₄, which showed 74% and 64% recovery, respectively (Table 3). Using the TPTZ-HCl method, we obtained comparable sucrose recovery but significantly lower laminarin recovery (65%) compared to the 94–99% recovery reported by Myklestad et al. (1997). These findings highlight that the TPTZ-op-H₂SO₄ method is better able to break glycosidic bonds to liberate glucose units compared to the TPTZ-HCl and TPTZ-H₂SO₄ methods. The PSA method results exhibited widely variable carbon recovery, ranging from 68% (laminarin) to 213% (sucrose). The comparable recoveries observed for laminarin and cellulose using both the TPTZ-HCl and TPTZ-H₂SO₄ methods indicate they have a similar efficiency in breaking down glycosidic bonds in glucose-based compounds. The lower recoveries from sucrose and raffinose

Table 2. Carbon recovery of monosaccharide standards (R_c , mean %, coefficient of variation in parentheses, $n = 3$) hydrolyzed by our optimized hydrolysis method and measured by TPTZ after alkalization (TPTZ-op-H₂SO₄), PSA method, and TPTZ method without hydrolysis.

Type of carbohydrate	Name	TPTZ-op-H ₂ SO ₄	PSA	TPTZ*
Aldohexoses	D-(+)-Galactose	93.57 (0.97)	58.25 (24.58)	96
	D-(+)-Mannose	99.26 (3.39)	66.07 (11.72)	95
Deoxysugars	D-(+)-Fucose	79.19 (1.70)	117.81 (2.14)	74
	L-Rhamnose	101.37 (3.84)	71.66 (4.43)	79
Ketohexoses	D-(−)-Fructose	43.77 (10.28)	162.07 (6.70)	103
Aldopentoses	D-Ribose	92.43 (5.00)	38.27 (13.37)	89
	D-(+)-Xylose	104.39 (0.89)	74.20 (12.59)	105
	L-(+)-Arabinose	102.42 (2.85)	37.67 (35.65)	88
Uronic acid	D-(+)-Glucuronic acid	100.2 (0.36)	33.19 (71.98)	95
	D-(+)-Galacturonic acid monohydrate	83.61 (7.85)	20.85 (21.61)	71
	D-Mannuronic acid	98.47 (2.22)	–	51
Amino sugar	<i>N</i> -Acetyl-D-glucosamine	88.75 (3.56)	<LOD	–
Average		90.6 (19.2)	61.8 (74.0)	86 (18.6)

*Reported by Myklestad et al. (1997).

Table 3. Carbon recovery of oligo- and polysaccharide standards (R_c , mean %, coefficient of variation in parenthesis, $n = 3$) hydrolyzed by our optimized hydrolysis method and measured by TPTZ after alkalization (TPTZ-op- H_2SO_4), hydrolysis by 0.1 mol L^{-1} HCl for 20 h at 100°C (TPTZ-HCl) and by 1.2 mol L^{-1} H_2SO_4 for 3 h at 100°C (TPTZ- H_2SO_4), PSA method.

Name	TPTZ-op- H_2SO_4	TPTZ-HCl	TPTZ- H_2SO_4	PSA
Sucrose	75.26 (5.18)	80.62 (4.92)	62.98 (7.35)	213.03 (1.42)
Raffinose pentahydrate	78.98 (6.41)	60.70 (10.40)	46.08 (12.83)	124.24 (0.85)
Laminarin	90.16 (4.44)	65.28 (10.63)	78.46 (1.08)	68.41 (15.77)
Amylose	92.45 (3.19)	96*	–	85.34 (7.92)
a-cellulose	88.59 (2.38)	68.13 (14.59)	68.64 (7.04)	103.89 (2.11)
Alginate	65.38 (2.42)	23.06 (3.04)	–	18.25 (87.95)
Pectin	89.00 (1.58)	86.18 (2.21)	–	38.85 (45.17)
Chitin	76.68 (1.55)	–	–	<LOD
Average	82.1 (11.5)	68.6 (34.5)	64.0 (21.2)	81.5 (83.3)

*Reported by Mykkestad et al. (1997), corrected based on the recovery of glucose.

indicate that TPTZ- H_2SO_4 might reduce the recovery of fructose and galactose more than the TPTZ-HCl method. Based on this observation, the TPTZ- H_2SO_4 method was excluded from further tests of the recovery of other polysaccharides. The optimized method exhibited a recovery of 65% from alginate and 89% from pectin, whereas TPTZ-HCl exhibited 23% and 86% recovery, respectively. PSA generally resulted in lower carbon recovery from uronic acid-containing polysaccharides, such as 18% from alginate and 39% from pectin. In addition, PSA could not detect polysaccharides of the amino sugar type, for instance, chitin.

Microalgae and marine particulate samples

Total particulate carbohydrate, measured as glucose equivalents, retrieved from phytoplankton cultures (diatoms: *M. polymorphus*, *T. pseudonana*; coccolithophore: *E. huxleyi*) and Bedford Basin particulate seawater samples ranged from 0.6 to 6.7 times higher using our optimized method compared

Table 4. Total particulate carbohydrate from laboratory cultures (pg cell^{-1}) and Bedford Basin field samples ($\mu\text{g L}^{-1}$) quantitated by TPTZ-op- H_2SO_4 (optimized hydrolysis method, hydrolysate alkalized and measured by TPTZ), PSA, and their ratio. Values in parentheses indicate one standard deviation ($n = 8$).

Sample type	TPTZ-op- H_2SO_4	PSA	TPTZ-op- H_2SO_4 /PSA
<i>Minutocellus polymorphus</i>	1.82 (0.02)	1.01 (0.01)	1.8
<i>Thalassiosira pseudonana</i>	20.43 (0.33)	10.25 (0.96)	2.0
<i>Emiliana huxleyi</i> (41.10 Pa pCO_2)	6.07 (0.17)	3.76 (0.15)	1.6
<i>E. huxleyi</i> (2.7 Pa pCO_2)	23.13 (0.69)	3.00 (0.24)	7.7
Bedford Basin	335.08 (3.56)	190.25 (0.95)	1.8

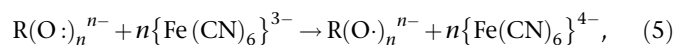
to the PSA method (Table 4). The Bedford Basin sample, collected during the March spring bloom dominated by diatoms, exhibited a similar discrepancy in carbohydrate recovery between the two methods, mirroring the results observed in the diatom samples.

Discussion

Carbohydrates represent about 8–10% of particulate organic carbon in the surface ocean, up to 30% in sediment, and 15–50% of the carbon in dissolved organic matter/or carbon (as reviewed by Bligh et al. 2022). Reliable quantification of the carbon content of carbohydrate in dissolved and particulate marine samples is useful for improving our understanding of the marine carbon cycle, including organic carbon production, remineralization, trophic transfer, and storage, as well as transformations into the dissolved organic matter pool. The TPTZ method was developed to be a rapid and precise method for quantifying dissolved carbohydrate, which has been adapted for use on particulate samples when coupled with hydrolysis of oligo- and polysaccharides. Carbohydrate quantification by TPTZ has similar accuracy compared to the more challenging MBTH method and compared to the PSA method is much more accurate for carbon recovery from mixtures of sugars. The TPTZ method is thought to quantify carbohydrates by using the reducing potential of a single aldehyde group present in reducing sugars to reduce ferricyanide (Mykkestad et al. 1997). Since hydrolyzed and unhydrolyzed monosaccharides possess a single aldehyde group, one might expect consistent recovery across sugars and hydrolysis conditions based on this mechanism. Contrary to expectations, we found that the TPTZ method can detect both hydroxyl and aldehyde groups in monosaccharides. In addition, we observed that the pH of the solution during the reduction of ferricyanide affects the yield. We varied hydrolysis conditions and the amount of base added before analysis, testing methodological variants across a

range of mono-, oligo-, and polysaccharides to develop our optimized hydrolysis protocol. Harsh hydrolysis conditions result in low recovery due to monosaccharide dehydration, whereas weak hydrolysis conditions lead to low recovery because polysaccharides are incompletely cleaved into their monosaccharide subunits. Insufficient alkalization of the hydrolysate leads to incomplete recovery of monosaccharides due to incomplete deprotonation, which prevents the maximum reduction of ferricyanide, resulting in lower molar absorptivity.

Acid dehydration of glucose into furfural eliminates three hydroxyl groups, leaving one aldehyde and one hydroxyl group on the furan ring (Fig. 1; Ranoux et al. 2013). If TPTZ solely detects aldehyde groups, we would anticipate no impact from dehydration. However, we observed a reduced molar absorptivity of the TPTZ-Fe²⁺ complex generated from dehydrated glucose, to approximately one third of the amount produced from unhydrolyzed glucose (Fig. 2a; Table 1). The observed reduction in molar absorptivity strongly suggests that the loss of hydroxyl groups results in the loss of colored TPTZ-Fe²⁺ complex. We propose that both aldehyde and hydroxyl groups contribute to the reduction of ferricyanide:



where the variable n in Eq. 5 is the number of ferricyanide molecules reduced in the reaction, that is, the number of reducing groups in the reducing sugar. Myklestad et al. (1997) reported varying glucose-equivalent recovery rates when using the TPTZ method with hydrolysis: 96–103% from aldohexoses, 103% from ketohexoses, 74–79% from deoxysugars, 88–105% from aldopentoses, and 51–95% from uronic acids. These sugars possess different numbers of reducing groups: aldohexoses and ketohexoses have 5–6, deoxysugars, aldopentoses and uronic acids have 4–5, depending on their cyclic or acyclic structures. This observed recovery pattern is consistent with the hypothesis that both aldehyde and hydroxyl groups contribute to the reduction of ferricyanide. Yields from the MBTH method are also affected by glucose dehydration. Pretreatment with 12 mol L⁻¹ H₂SO₄ followed by hydrolysis in 1.2 mol L⁻¹ H₂SO₄ at 100°C for 3 h resulted in a 50% decrease in the measured molar absorptivity by MBTH relative to unhydrated glucose (see fig. 1 in Pakulski and Benner 1992).

Hydrolysis is required to break oligo- and polysaccharides into their constituent monosaccharides for analysis, but harsh hydrolysis conditions will dehydrate carbohydrates, decreasing the number of reducing groups, production of the TPTZ-Fe²⁺ complex and recovery of carbohydrate, demonstrating a need for an optimized hydrolysis protocol for the analysis of total and dissolved particulate carbohydrate. Our optimized hydrolysis along with the alkalization of hydrolysate before TPTZ analysis achieved an average recovery of monosaccharides quantified relative to glucose of 94% and a more

consistent recovery (80–100%) from 11 out of 12 tested monosaccharides. Our optimized hydrolysis broke more glycosidic bonds in polysaccharides compared with using 0.1 mol L⁻¹ HCl for 20 h at 100°C (Myklestad et al. 1997) and 1.2 mol L⁻¹ H₂SO₄ for 3 h at 100°C (Hung et al. 2003) resulting in increased recovery. The mild concentration of HCl (0.1 mol L⁻¹) used by Myklestad et al. (1997) effectively broke α (1 → 4) glycosidic bonds in amylose and did not cause substantial dehydration in fructose. It resulted in similar recovery from sucrose and raffinose compared to our optimized hydrolysis; however, its low molarity was insufficient to fully liberate glucose from laminarin and cellulose. Alginate had the lowest recovery among the polysaccharide standards using the optimized method (65%), but this recovery was significantly higher than the 23% obtained using 0.1 mol L⁻¹ HCl at 100°C for 20 h (TPTZ-HCl). There are no perfect hydrolysis conditions for all sugars; our choice is a trade-off aimed at increasing total carbohydrate recovery, ensuring adequate recovery for most sugars, and limiting the loss of alginate and fructose.

Carbohydrate recovery is predictably influenced by factors such as the number of carbon atoms and reducing groups in a sugar and the composition of monosaccharides within an oligo- or polysaccharide. For example, the recovery of pectin using both the optimized method (89% ± 2%) and 0.1 mol L⁻¹ HCl at 100°C for 20 h (TPTZ-HCl, 86% ± 2%) aligned closely with the recovery of galacturonic acid, the principal component of pectin (84% ± 8%). This similarity supports the hypothesis that the maximum recovery is constrained by the four reducing groups in cyclic galacturonic acid. Self-catalyzed dehydration of fructose resulted in a 50% decrease in the number of reducing groups and only 44% ± 5% recovery relative to glucose (Fig. 8). The dehydration of fructose during the hydrolysis stage limits recovery of sucrose and raffinose (Table 3). Complete hydrolysis of sucrose (into glucose and fructose) and raffinose (into galactose, glucose, and fructose) leads us to predict recoveries of 72% and 79%, respectively, based on the 44% and 94% observed recovery of fructose and galactose equivalent to glucose (Table 2). These predictions closely matched the observed recoveries of 75% ± 5% and 79% ± 6%.

The optimized method improves recovery of many monosaccharides in neutralized solutions (Table 2, relative to Myklestad et al. 1997) by alkalizing hydrolyzed carbohydrates before the TPTZ reaction. We attribute this result to the complete deprotonation of reducing groups and complete color development of the TPTZ-Fe²⁺ complex. The ferricyanide reduction activity of hydroxyl groups depends on the proton affinity and acidity constant. Feng et al. (2013) demonstrated complete deprotonation of cyclic D-β-glucopyranose in an alkaline solution (pH 11), which is like the alkaline environment of the ferricyanide reagent in the TPTZ method. As a result, all the hydroxyl groups in glucose will exhibit similar

reductive properties to the aldehyde group in reducing ferricyanide. Variation in carbohydrate quantitation also arises since monosaccharides are quantified relative to glucose. Cyclic D-β-glucopyranose can only reduce 83% (5/6) of the ferricyanide that would be reduced by the six reducing groups in acyclic D-glucose. The alkalized medium stabilizes glucose in a complete cyclic structure, consistently providing five reducing groups from glucose. Even if no hydrolysis is required, such as in the TPTZ analysis of dissolved monosaccharide, we recommend alkalizing carbohydrate samples to ensure equal yields across diverse monosaccharides (Hu and Finkel 2022a).

Our optimized method showed significant improvement compared to the PSA method which gave highly variable recovery from oligo- and polysaccharides, ranging from 38% for pectin to 213% for sucrose (Table 3). The concentrated H₂SO₄ used in the PSA method resulted in a more comprehensive hydrolysis of cellulose but not amylose and laminarin. This disparity may be attributed to the polymerization of furan derivatives from more easily broken glycosidic bonds. The PSA method generally yields lower recovery from uronic acid and fails to detect polysaccharides of the amino sugar type, such as chitin. We expect that our optimized carbohydrate hydrolysis along with hydrolysate alkalization will enhance the TPTZ-based carbohydrate analysis, resulting in increased carbohydrate yield and reproducibility compared to both PSA method and TPTZ method measuring carbohydrates hydrolyzed by common hydrolysis (Tables 2, 3). We obtain greatly increased carbohydrate yields from phytoplankton cultures and field samples (Table 4). The diatom *T. pseudonana* contains chrysolaminarin (a linear polymer of β (1 → 3) and β (1 → 6) linked glucose units) and a chitin-based scaffold associated with the frustule (Brunner et al. 2009). Laminarin recovery increased 30% with our method relative to PSA and chitin was undetectable with PSA. The coccolithophore *E. huxleyi* is known to have uronic acids (Lee et al. 2016) which are poorly recovered by PSA (21–38%) compared to our optimized method (84–100%). The carbohydrate matrix in *E. huxleyi* grown at 2.7 Pa pCO₂ shifts from glucose to mannose, galactose and arabinose compared with cultures grown at high pCO₂ (Borchard and Enge 2012). The carbohydrate composition of *E. huxleyi* and low recovery from galactose (58%), mannose (66%), arabinose (38%), and uronic acid (21–38%) using the PSA method, may explain the twofold to eightfold increase in carbohydrate recovery in this species with our method relative to PSA. Similarly, we anticipate increased yield of carbohydrates in *Phaeocystis* due to its pectin-like polysaccharides (Alderkamp et al. 2007) and bacteria-produced alginic acids (Usov 1999) relative to PSA.

We did not investigate the quantitation of sulfated carbohydrates. Acid hydrolysis might cleave the sulfate ester linkages in sulfated glycans (Kim et al. 2023), liberating monosaccharides and potentially restoring reducing groups. The efficiency of desulfation during hydrolysis can vary, so further

research is needed to determine the applicability and accuracy of methods investigated here for these compounds.

Conclusions

TPTZ analysis measures both hydroxyl and aldehyde groups, contingent upon full deprotonation in an alkaline medium for complete color development. Dehydration during hydrolysis reduces the number of reducing groups, resulting in lower molar absorptivity and recovery. Insufficient alkalization before TPTZ analysis results in incomplete and variable recovery of monosaccharide mixtures. To address these challenges, we recommend an optimized method for quantifying total particulate carbohydrate: (1) vortex samples in 9 mol L⁻¹ H₂SO₄ for 15 s, (2) dilute to 1.6 mol L⁻¹ H₂SO₄ and hydrolyze at 90°C for 3 h, (3) add 12 mol L⁻¹ NaOH to the hydrolysate for a final ratio of 0.82 ([H⁺] from hydrolysate to [OH⁻] from NaOH), (4) conduct TPTZ analysis. Our optimized method (Hu and Finkel 2022a,b) significantly improves the recovery of various mono-, oligo-, and polysaccharides relative to previously published TPTZ protocols measuring carbohydrates hydrolyzed by common hydrolysis, enhancing average recovery rates to 90% and results in improved reproducibility compared to the PSA method. The enhanced accuracy of our method will facilitate better estimates of particulate and dissolved carbohydrates in biological and environmental samples.

References

- Alderkamp, A.-C., A. G. J. Buma, and M. van Rijssel. 2007. The carbohydrates of *Phaeocystis* and their degradation in the microbial food web. *Biogeochemistry* **83**: 99–118. doi:10.1007/s10533-007-9078-2
- Andreeva, A., E. Budenkova, O. Babich, S. Sukhikh, V. Dolganyuk, P. Michaud, and S. Ivanova. 2021. Influence of carbohydrate additives on the growth rate of microalgae biomass with an increased carbohydrate content. *Mar. Drugs* **19**: 381–399. doi:10.3390/md19070381
- Arnosti, C., M. Wietz, T. Brinkhoff, J.-H. Hehemann, D. Probandt, L. Zeugner, and R. Amann. 2021. The biogeochemistry of marine polysaccharides: Sources inventories, and bacterial drivers of the carbohydrate cycle. *Ann. Rev. Mar. Sci.* **13**: 81–108. doi:10.1146/annurev-marine-032020-012810
- Avigad, G. 1975. Colorimetric ultramicro assay for reducing sugars, p. 27, 27–29, 29. In W. A. Wood [ed.], *Methods in enzymology*, v. **41**. Academic Press. doi:10.1016/S0076-6879(75)41006-0
- Becker, S., J. Tebben, S. Coffinet, K. Wiltshire, M. H. Iversen, T. Harder, K.-U. Hinrichs, and J.-H. Hehemann. 2020. Laminarin is a major molecule in the marine carbon cycle. *Proc. Natl. Acad. Sci. USA* **117**: 6599–6607. doi:10.1073/pnas.1917001117

- Berges, J. A., D. J. Franklin, and P. J. Harrison. 2001. Evolution of an artificial seawater medium: Improvements in enriched seawater artificial water over the last two decades. *J. Phycol.* **37**: 1138–1145. doi:[10.1046/j.1529-8817.2001.01052.x](https://doi.org/10.1046/j.1529-8817.2001.01052.x)
- Biersmith, A., and R. Benner. 1998. Carbohydrates in phytoplankton and freshly produced dissolved organic matter. *Mar. Chem.* **63**: 131–144. doi:[10.1016/S0304-4203\(98\)00057-7](https://doi.org/10.1016/S0304-4203(98)00057-7)
- Bligh, M., N. Nguyen, H. Buck-Wiese, S. Vidal-Melgosa, and J.-H. Hehemann. 2022. Structures and functions of algal glycans shape their capacity to sequester carbon in the ocean. *Curr. Opin. Chem. Biol.* **71**: 102204. doi:[10.1016/j.cbpa.2022.102204](https://doi.org/10.1016/j.cbpa.2022.102204)
- Borch, N. H., and D. L. Kirchman. 1997. Concentration and composition of dissolved combined neutral sugars (polysaccharides) in seawater determined by HPLC-PAD. *Mar. Chem.* **57**: 85–95. doi:[10.1016/S0304-4203\(97\)00002-9](https://doi.org/10.1016/S0304-4203(97)00002-9)
- Borchard, C., and A. Enge. 2012. Organic matter exudation by *Emiliania huxleyi* under simulated future ocean conditions. *Biogeoscience* **9**: 1199–1236. doi:[10.5194/bgd-9-1199-2012](https://doi.org/10.5194/bgd-9-1199-2012)
- Brown, M. R. 1991. The amino-acid and sugar composition of 16 species of microalgae used in mariculture. *J. Exp. Mar. Biol. Ecol.* **145**: 79–99. doi:[10.1016/0022-0981\(91\)90007-J](https://doi.org/10.1016/0022-0981(91)90007-J)
- Brunner, E., P. Richtighammer, H. Ehrlich, S. Paasch, P. Simon, S. Ueberlein, and K.-H. van Pée. 2009. Chitin-based organic networks: An integral part of cell wall biosilica in the diatom *Thalassiosira pseudonana*. *Angew. Chem. Int. Ed.* **48**: 9724–9727. doi:[10.1002/anie.200905028](https://doi.org/10.1002/anie.200905028)
- Burney, C. M., and J. M. N. Sieburth. 1977. Dissolved carbohydrates in seawater. II, A spectrophotometric procedure for total carbohydrate analysis and polysaccharide estimation. *Mar. Chem.* **5**: 15–28. doi:[10.1016/0304-4203\(77\)90012-3](https://doi.org/10.1016/0304-4203(77)90012-3)
- Chanudet, V., and M. Filella. 2006. The application of the MBTH method for carbohydrate determination in freshwaters revisited. *Int. J. Environ. Anal. Chem.* **86**: 693–712. doi:[10.1080/03067310600585936](https://doi.org/10.1080/03067310600585936)
- Chen, W., L. Gao, L. Song, M. Sommerfeld, and Q. Hu. 2023. An improved phenol-sulfuric acid method for the quantitative measurement of total carbohydrates in algal biomass. *Algal Res.* **70**: 102986. doi:[10.1016/j.algal.2023.102986](https://doi.org/10.1016/j.algal.2023.102986)
- Crompton, T. R. 2006. Analysis of seawater: A guide for the analytical and environmental chemist. Springer. doi:[10.1007/b138036](https://doi.org/10.1007/b138036)
- Deschamps, P., and others. 2008. The heterotrophic dinoflagellate *Cryptothecodinium cohnii* defines a model genetic system to investigate cytoplasmic starch synthesis. *Eukaryot. Cell* **7**: 872–880. doi:[10.1128/ec.00461-07](https://doi.org/10.1128/ec.00461-07)
- Dubois, M., K. Gilles, J. K. Hamilton, P. A. Rebers, and F. Smith. 1951. A colorimetric method for the determination of sugars. *Nature* **168**: 167. doi:[10.1038/168167a0](https://doi.org/10.1038/168167a0)
- Engel, A., and N. Händel. 2011. A novel protocol for determining the concentration and composition of sugars in particulate and in high molecular weight dissolved organic matter (HMW-DOM) in seawater. *Mar. Chem.* **127**: 180–191. doi:[10.1016/j.marchem.2011.09.004](https://doi.org/10.1016/j.marchem.2011.09.004)
- Fazio, S. A., E. J. Uhlinger, J. H. Parker, and D. C. White. 1982. Estimations of uronic acids as quantitative measures of extracellular and cell wall polysaccharide polymers from environmental samples. *Appl. Environ. Microbiol.* **43**: 1151–1159. doi:[10.1128/aem.43.5.1151-1159.1982](https://doi.org/10.1128/aem.43.5.1151-1159.1982)
- Fearon, W. R. 2014. The carbohydrates, or glucides, p. 76–101. *In* An introduction to biochemistry. Academic Press. doi:[10.1016/B978-1-4832-0036-1.50013-6](https://doi.org/10.1016/B978-1-4832-0036-1.50013-6)
- Feng, S., C. Bagia, and G. Mpourmpakis. 2013. Determination of proton affinities and acidity constants of sugars. *Chem. A Eur. J.* **117**: 5211–5219. doi:[10.1021/jp403355e](https://doi.org/10.1021/jp403355e)
- Gandini, A. 1997. Furans in polymer chemistry. *Prog. Polym. Sci.* **22**: 1203–1379. doi:[10.1016/S0079-6700\(97\)00004-x](https://doi.org/10.1016/S0079-6700(97)00004-x)
- Guillard, R. R. L., and J. H. Ryther. 1962. Studies of marine planktonic diatoms: I. *Cyclotella nana* Hustedt and *Detonula confervacea* (Cleve) Gran. *Can. J. Microbiol.* **8**: 229–239. doi:[10.1139/m62-029](https://doi.org/10.1139/m62-029)
- Hallegraeff, G. M., D. M. Anderson, A. D. Cembella, and H. O. Enevoldsen. 2004. Manual on harmful marine microalgae, 2nd Edition. UNESCO.
- Handa, N. 1966. Examination on the applicability of the phenol sulfuric acid method to the determination of dissolved carbohydrate in sea water. *J. Oceanogr. Soc. Jpn* **22**: 79–86. doi:[10.5928/kaiyou1942.22.79](https://doi.org/10.5928/kaiyou1942.22.79)
- Haug, A., and B. Larsen. 1965. A study on the constitution of alginic acid by partial acid hydrolysis, p. 271–277. *In* E. G. Young and J. L. McLachlan [eds.], Proceedings of the Fifth International Seaweed Symposium. Pergamon. doi:[10.1016/b978-0-08-011841-3.50043-4](https://doi.org/10.1016/b978-0-08-011841-3.50043-4)
- Hedges, J. I., J. A. Baldock, Y. Gélinas, C. Lee, M. Peterson, and S. G. Wakeham. 2001. Evidence for non-selective preservation of organic matter in sinking marine particles. *Nature* **409**: 801–804. doi:[10.1038/35057247](https://doi.org/10.1038/35057247)
- Hickey, R. M. 2012. Extraction and characterization of bioactive carbohydrates with health benefits from marine resources: Macro- and microalgae, cyanobacteria, and invertebrates, p. 159–172. *In* M. Hayes [ed.], Marine bioactive compounds. Springer. doi:[10.1007/978-1-4614-1247-2_6](https://doi.org/10.1007/978-1-4614-1247-2_6)
- Hu, X., S. Jiang, L. Wu, S. Wang, and C.-Z. Li. 2017. One-pot conversion of biomass-derived xylose and furfural into levulinic esters via acid catalysis. *Chem. Commun.* **53**: 2938–2941. doi:[10.1039/C7CC01078H](https://doi.org/10.1039/C7CC01078H)
- Hu, Y. Y., and Z. V. Finkel. 2022a. Measurement of dissolved carbohydrate. *Protocols.io*. doi:[10.17504/protocols.io.bp2l6168zvqe/v1](https://doi.org/10.17504/protocols.io.bp2l6168zvqe/v1)
- Hu, Y. Y., and Z. V. Finkel. 2022b. Total particulate carbohydrate from microalgae. *Protocols.io*. doi:[10.17504/protocols.io.yxmvkmk24ng3p/v1](https://doi.org/10.17504/protocols.io.yxmvkmk24ng3p/v1)

- Hung, C.-C., L. Guo, P. H. Santschi, N. Alvarado-Quiroz, and J. M. Haye. 2003. Distribution of carbohydrate species in the Gulf of Mexico. *Mar. Chem.* **81**: 119–135. doi:10.1016/S0304-4203(3)00012-4
- Itagaki, H. 1994. Saccharification process of cellulose in 97% sulfuric acid monitored by sulfuric acid induced ultraviolet absorption behaviour. *Polymer* **35**: 50–52. doi:10.1016/0032-3861(94)90048-5
- Jochum, C., P. Jochum, and B. R. Kowalski. 1981. Error propagation and optimal performance in multicomponent analysis. *Anal. Chem.* **53**: 85–92. doi:10.1021/ac00224a023
- Kamerling, J. P., and G. J. Gerwig. 2007. Strategies for the structural analysis of carbohydrates, p. 1–68. *In* H. Kamerling [ed.], *Comprehensive glycoscience*. Elsevier. doi:10.1016/B978-044451967-2/00032-5
- Kim, S. B., M. Farrag, S. K. Mishra, S. K. Misra, J. S. Sharp, R. J. Doerksen, and V. H. Pomin. 2023. Selective 2-desulfation of tetrasaccharide-repeating sulfated fucans during oligosaccharide production by mild acid hydrolysis. *Carbohydr. Polym.* **301**: 120316. doi:10.1016/j.carbpol.2022.120316
- Latil de Ros, D. 2017. Microalgae as a new source of chitosans. PhD thesis. Universitat de Barcelona.
- Laurens, L. M. L., and others. 2012. Algal biomass constituent analysis: Method uncertainties and investigation of the underlying measuring chemistries. *Anal. Chem.* **84**: 1879–1887. doi:10.1021/ac202668c
- Lee, R. B. Y., D. A. I. Mavridou, G. Papadakos, H. I. O. McClelland, and R. E. M. Rickaby. 2016. The uronic acid content of coccolith-associated polysaccharides provides insight into coccolithogenesis and past climate. *Nat. Commun.* **7**: 13144. doi:10.1038/ncomms13144
- Mellmer, M. A., and others. 2019. Effects of chloride ions in acid-catalyzed biomass dehydration reactions in polar aprotic solvents. *Nat. Commun.* **10**: 1132. doi:10.1038/s41467-019-09090-4
- Mopper, K. 1977. Sugars and uronic acids in sediment and water from the Black Sea and North Sea with emphasis on analytical techniques. *Mar. Chem.* **5**: 585–603. doi:10.1016/0304-4203(77)90044-5
- Mulder, G. J. 1840. Untersuchungen über die Humussubstanzen. *J. Prakt. Chem.* **21**: 203–240. doi:10.1002/prac.18400210121
- Myklestad, S. M., E. Skånøy, and S. Hestmann. 1997. A sensitive and rapid method for analysis of dissolved mono- and polysaccharides in seawater. *Mar. Chem.* **56**: 279–286. doi:10.1016/S0304-4203(96)00074-6
- Niaz, K., F. Khan, and M. A. Shan. 2020. Analysis of carbohydrates (monosaccharides, polysaccharides), p. 621–633. *In* A. S. Silva, S. F. Nabavi, M. Saeedi, and S. M. Nabavi [eds.], *Recent advances in natural products analysis*. Elsevier. doi:10.1016/B978-0-12-816455-6.00018-4
- Pakulski, J. D., and R. Benner. 1992. An improved method for the hydrolysis and MBTH analysis of dissolved and particulate carbohydrates in seawater. *Mar. Chem.* **40**: 143–160. doi:10.1016/0304-4203(92)90020-b
- Panagiotopoulos, C., and R. Sempéré. 2005. Analytical methods for the determination of sugars in marine samples: A historical perspective and future directions. *Limnol. Oceanogr.: Methods* **3**: 419–454. doi:10.4319/lom.2005.3.419
- Passos, F., E. Uggetti, H. Carrère, and I. Ferrer. 2015. Algal biomass: Physical pretreatments, p. 195–226. *In* A. Pandey, S. Negi, P. Binod, and C. Larroche [eds.], *Pretreatment of biomass*. Elsevier. doi:10.1016/B978-0-12-800080-9.00011-6
- Priest, T., S. Vidal-Melgosa, J. H. Hehemann, R. Amann, and B. M. Fuchs. 2023. Carbohydrates and carbohydrate degradation gene abundance and transcription in Atlantic waters of the Arctic. *ISME Commun.* **3**: 130. doi:10.1038/s43705-023-00324-7
- Ramli, R. N., C. K. Lee, and M. K. Kassim. 2020. Extraction and characterization of starch from microalgae and comparison with commercial corn starch. *IOP Conf. Ser.: Mater. Sci. Eng.* **716**: 012012. doi:10.1088/1757-899x/716/1/012012
- Ranoux, A., K. Djanashvili, I. W. C. E. Arends, and U. Hanefeld. 2013. 5-Hydroxymethylfurfural synthesis from hexoses is autocatalytic. *ACS Catal.* **3**: 760–763. doi:10.1021/cs400099a
- Rizelio, V. M., L. V. Gonzaga, G. D. S. C. Borges, G. A. Micks, R. Fett, and A. C. O. Costa. 2012. Development of a fast MECK method for determination of 5-HMF in honey samples. *Food Chem.* **113**: 1640–1645. doi:10.1016/j.foodchem.2011.11.058
- Romankevich, E. A., and V. E. Artem'ev. 1969. Composition of the organic matter of sediments from the Kuril-Kamchatka Trench. *Oceanology* **9**: 644–653. doi:10.1594/PANGAEA.758722
- Rosenau, T., and others. 2017. Chromophores from hexeneuronic acids: Identification of HexA-derived chromophores. *Cellulose* **24**: 3671–3687. doi:10.1007/s10570-017-1397-4
- Sarazin, C., N. Delaunay, C. Costanza, V. Eudes, J.-M. Mallet, and P. Gareil. 2011. New avenue for mid-UV-range detection of underivatized carbohydrates and amino acids in capillary electrophoresis. *Anal. Chem.* **83**: 7381–7387. doi:10.1021/ac2012834
- Schievano, E., M. Tonoli, and F. Rastrelli. 2017. NMR quantification of carbohydrates in complex mixtures. A challenge on honey. *Anal. Chem.* **89**: 13405–13414. doi:10.1021/acs.analchem.7b03656
- Selvendran, R. R., J. F. March and S. G. Ring. 1979. Determination of aldoses and uronic acid content of vegetable fiber. *Anal. Biochem.* **96**: 282–292. doi:10.1016/0003-2697(79)90583-9
- Speakman, P. T., and W. A. Waters. 1955. Kinetic features of the oxidation of aldehydes ketones, and nitroparaffins with alkaline ferricyanide. *J. Chem. Soc.*: 40–45. doi:10.1039/jr9550000040

- Swain, F. M., and J. M. Bratt. 1972. Comparative carbohydrate geochemistry of bay, salt marsh, and deep gulf sediments. *In* Comparative carbohydrate geochemistry of bay, salt marsh and deep gulf sediments. Sea Grant Publication.
- Tornabene, T. G., T. F. Bourne, S. Raziuddin, and A. Ben-Amotz. 1985. Lipids and lipopolysaccharide constituents of cyanobacterium *Spirulina platensis* (Cyanophyceae, Nostocales). *Mar. Ecol. Prog. Ser.* **22**: 121–125. doi:10.3354/meps022121
- Usov, A. I. 1999. Alginic acids and alginates: Analytical methods used for their estimation and characterization of composition and primary structure. *Russ. Chem. Rev.* **68**: 957–966. doi:10.1070/RC1999v068n11ABEH000532
- van Oijen, T., M. J. W. Veldhuis, M. Y. Gorbunov, J. Nishioka, M. A. van Leeuwe, and H. J. W. de Baar. 2005. Enhanced carbohydrate production by Southern Ocean phytoplankton in response to in situ iron fertilization. *Mar. Chem.* **93**: 33–52. doi:10.1016/j.marchem.2004.06.039
- van Wychen, S., W. Long, S. K. Black, and L. M. L. Laurens. 2017. MBTH: A novel approach to rapid spectrophotometric quantitation of total algal carbohydrates. *Anal. Biochem.* **518**: 90–93. doi:10.1016/j.ab.2016.11.014
- Vidal-Melgosa, S., and others. 2021. Diatom fucan polysaccharide precipitates carbon during algal blooms. *Nat. Commun.* **12**: 1150. doi:10.1038/s41467-021-21009-6
- Wang, S., and L. Copeland. 2015. Effect of acid hydrolysis on starch structure and functionality: A review. *Crit. Rev. Food Sci. Nutr.* **55**: 1081–1097. doi:10.1080/10408398.2012.684551
- Wang, C., Y. Hou, Y. Lin, Y. Xie, D. Wei, N. Zhou, and H. He. 2018. Rapid determination and conversion study of 5-hydroxymethylfurfural and its derivatives in glucose injection. *New J. Chem.* **42**: 17725–17731. doi:10.1039/c8nj03019g

Acknowledgments

We thank Khadijah Carey, Nuwanthi Samarasinghe, and Dr. Yong Zhang for providing live culture samples. We appreciate Magdalena Wacławik (Program Manager) and Tamara Wilson (Field Technician) for Bedford Basin Time Series sampling (in partnership with the Department of Fisheries and Oceans). We express our gratitude to the Associate Editor and three anonymous reviewers for their feedback, which has enhanced the quality of our manuscript. This work was supported by the Simons Collaboration on Computational Biogeochemical Modeling of Marine Ecosystems (CBIOMES, Grant 549937 to Z.V.F.) and the Simons Collaborative on Ocean Processes and Ecology (SCOPE-Gradients, Grant 723789 to Z.V.F.).

Submitted 28 September 2023

Revised 15 March 2024

Accepted 20 March 2024

Associate editor: Krista Longnecker